doi:10.1016/j.jmb.2010.07.053 J. Mol. Biol. (2010) 402, 539–551

Contents lists available at www.sciencedirect.com

Journal of Molecular Biology

journal homepage: http://ees.elsevier.com.jmb

Urate Is a Ligand for the Transcriptional Regulator PecS

Inoka C. Perera and Anne Grove*

Department of Biological Sciences, Louisiana State University, Baton Rouge, LA 70803, USA

Received 7 July 2010;
received in revised form
17 July 2010;
accepted 26 July 2010
Available online
1 August 2010

Edited by J. Karn

Keywords:
MarR;
PecS;
urate;
oxidative burst;
plant immunity

PecS is a member of the MarR (*m*ultiple *a*ntibiotic *r*esistance *r*egulator) family, which has been shown in *Erwinia* to regulate the expression of virulence genes. MarR homologs typically bind a small molecule ligand, resulting in attenuated DNA binding. For PecS, the natural ligand has not been identified. We have previously shown that urate is a ligand for the *Deinococcus radiodurans*-encoded MarR homolog HucR (*h*ypothetical *u*ricase *r*egulator) and identified residues responsible for ligand binding. We show here that all four residues involved in urate binding and propagation of conformational changes to DNA recognition helices are conserved in PecS homologs, suggesting that urate is the ligand for PecS. Consistent with this prediction, *Agrobacterium tumefaciens* PecS specifically binds urate, and urate attenuates DNA binding *in vitro*. PecS binds two operator sites in the intergenic region between the divergent *pecS* gene and *pecM* genes, one of which features two partially overlapping repeats to which PecS binds as a dimer on opposite faces of the duplex. Notably, urate dissociates PecS from cognate DNA, allowing transcription of both genes *in vivo*. Taken together, our data show that urate is a ligand for PecS and suggest that urate serves a novel function in signaling the colonization of a host plant.

Introduction

Plants are aerobic organisms. During the reduction of O_2 to H_2O, reactive oxygen species (ROS) are generated, and environmental stress conditions, including invading bacteria, result in overproduction of ROS as a defense mechanism. Several enzymes, including NADPH oxidase and xanthine oxidase, have been implicated in such ROS production; the latter participates in the catabolism of purines by converting hypoxanthine into xanthine and by converting xanthine into urate, and both reactions are associated with the production of ROS.[1–3]

Bacteria that interact with plants commonly need to alternate between a soil-dwelling saprophytic lifestyle and a symbiotic or pathogenic phase associated with colonization of the plant host. Examples include soil bacteria belonging to the order Rhizobiales, which invade legume roots to form nitrogen-fixing root nodules, and *Erwinia* species, which cause soft-rot diseases in a variety of plants.[4,5] The success of such bacterial species therefore depends on their ability to counter host defenses such as the production of ROS. Thus, production of antioxidants is vital for survival during host invasion. Among others, indigoidine has been shown to be an important antioxidant in a number of plant-pathogenic bacteria and has been best characterized in *Erwinia chrysanthemi* (*Dickeya dadantii*).[6] It was shown that indigoidine biosynthesis and secretion *via* the efflux pump PecM are regulated by the transcriptional regulator PecS.[7–9] Indeed, PecS regulates numerous genes that are essential for infectivity and disease progression, and is named for its regulation of pectinase gene expression in *Erwinia* sp.; pectinases are enzymes that play a significant role in the maceration of plant tissue, which gives rise to the characteristic symptoms.[10,11]

PecS belongs to the branch of the MarR (*m*ultiple *a*ntibiotic *r*esistance *r*egulator) family that is characterized by the ability to bind specific promoter

*Corresponding author. E-mail address: agrove@lsu.edu.

Abbreviations used: ROS, reactive oxygen species; EDTA, ethylenediaminetetraacetic acid; BSA, bovine serum albumin.

sequences (causing transcriptional repression) and the ability to associate with a small molecule ligand.[12] When the ligand is bound, derepression occurs to permit the expression of a regulon. For MarR, this means the expression of antibiotic resistance genes upon binding to antibiotics.[13–15] For PecS, it means the expression of a regulon associated with host colonization; however, the natural ligand has not been identified.[11,16]

As plants respond to invading bacteria by producing ROS, urate is generated as a byproduct.[17] However, urate is also a potent antioxidant that may be specifically produced in response to oxidative stress.[18–20] For example, cellular levels of endogenous urate are tightly regulated in *Deinococcus radiodurans*, a nonpathogenic bacterium known for its remarkable ability to withstand exposure to ionizing radiation and other sources of DNA damage, including that induced by oxidative stress.[21–24] We recently characterized the *D. radiodurans*-encoded MarR homolog HucR (*h*ypothetical *u*ricase *r*egulator), which functions as a transcriptional repressor, regulating its own expression and that of a divergent gene encoding a uricase.[25,26] Uricase catalyzes the conversion of urate to 5-hydroxyisourate, which is enzymatically or spontaneously broken down to allantoin.[27,28] Urate is the natural ligand for HucR, and *in vivo* studies have shown that when *D. radiodurans* is grown in the presence of urate, *hucR* and uricase transcripts are upregulated.[25]

We report here that urate is a ligand for the subset of MarR homologs previously annotated as PecS. Specifically, we show that *Agrobacterium tumefaciens* (*Rhizobium radiobacter*) encodes a PecS homolog whose repressor function is alleviated by urate both *in vitro* and *in vivo*. These data not only reveal the ligand for a critical transcription factor implicated in the bacterial colonization of host plants but also suggest a novel function for urate in signaling such colonization.

Results

Urate-coordinating residues are conserved in PecS homologs

We recently identified four residues involved in urate binding to HucR and in conferring attenuated DNA binding; while W20 and R80 of HucR directly coordinate urate, D73 is repelled by deprotonated urate, resulting in a movement of the DNA recognition helix that is otherwise held in place by a salt bridge between D73 and R106.[29] Alignment of the HucR amino acid sequence with that of other MarR homologs reveals the conservation of residues involved in coordinating urate and in communicating its binding to the DNA recognition helix in only a subset of these homologs, including PecS from the plant pathogens *E. chrysanthemi* and *A. tumefaciens* (Fig. 1a). Notably, proteins such as *Escherichia coli* MarR,[31] *Salmonella typhimurium* SlyA (Protein Data Bank ID 3DEU), and *Methanobacterium thermoautotrophicum* MTH313,[32] which respond to the ligand salicylate, do not conserve these residues; this is consistent with the observation that salicylate is not an efficient ligand for HucR.[25] What is also notable is that all residues are conserved on an all-or-none basis, consistent with their role in a common function.

As noted above, these plant pathogens encode a highly conserved genomic locus that includes the MarR homolog PecS. As is the case for other MarR homologs, divergently oriented genes are predicted to be repressed by the binding of PecS to the intergenic region, followed by derepression once the natural ligand is bound by PecS. In the plant pathogens, the locus includes PecM, a membrane protein with 10 predicted membrane-spanning segments that has been shown in *E. chrysanthemi* to be involved in the efflux of the antioxidant indigoidine.[7,9]

The annotated PecS homologs share a higher degree of sequence identity with HucR compared to other MarR homologs, with a 35.3% sequence identity between HucR and *A. tumefaciens* PecS and only an 18.4% identity between HucR and *E. coli* MarR. Accordingly, the HucR structure is identified by SWISS-MODEL as the appropriate structure on which to model PecS with less than 0.1 Å rmsd between C^{α} positions (Fig. 1c). A notable feature of HucR (and presumably of PecS) is the existence of an additional N-terminal helix not present in other homologs such as *E. coli* MarR and MTH313;[31,32] one of the urate-coordinating residues (W20 in HucR) protrudes from this N-terminal helix.

PecS binds a tandem palindrome

To determine whether urate indeed serves as a ligand for PecS homologs, we cloned *A. tumefaciens pecS*, expressed it in *E. coli*, and purified it to >95% homogeneity (Fig. 2a). Size-exclusion chromatography shows that PecS exists as a dimer of 43.7± 0.7 kDa (including 6× His tag) in solution, closely matching its theoretical molecular mass of 46.1 kDa (Fig. 2b). PecS has a melting temperature of 61.3± 0.5 °C, as determined by differential scanning fluorometry, using SYPRO Orange as fluorescent reporter for protein unfolding as a function of temperature (Fig. 2c). The thermal stability of PecS is comparable to that of other MarR homologs, all having relatively high melting temperatures compared to the physiological growth temperatures of the respective organisms.[25,33]

HucR binds a 9 bp imperfect inverted repeat.[25] Accordingly, PecS was predicted to bind an identified 9 bp inverted repeat in the intergenic region of

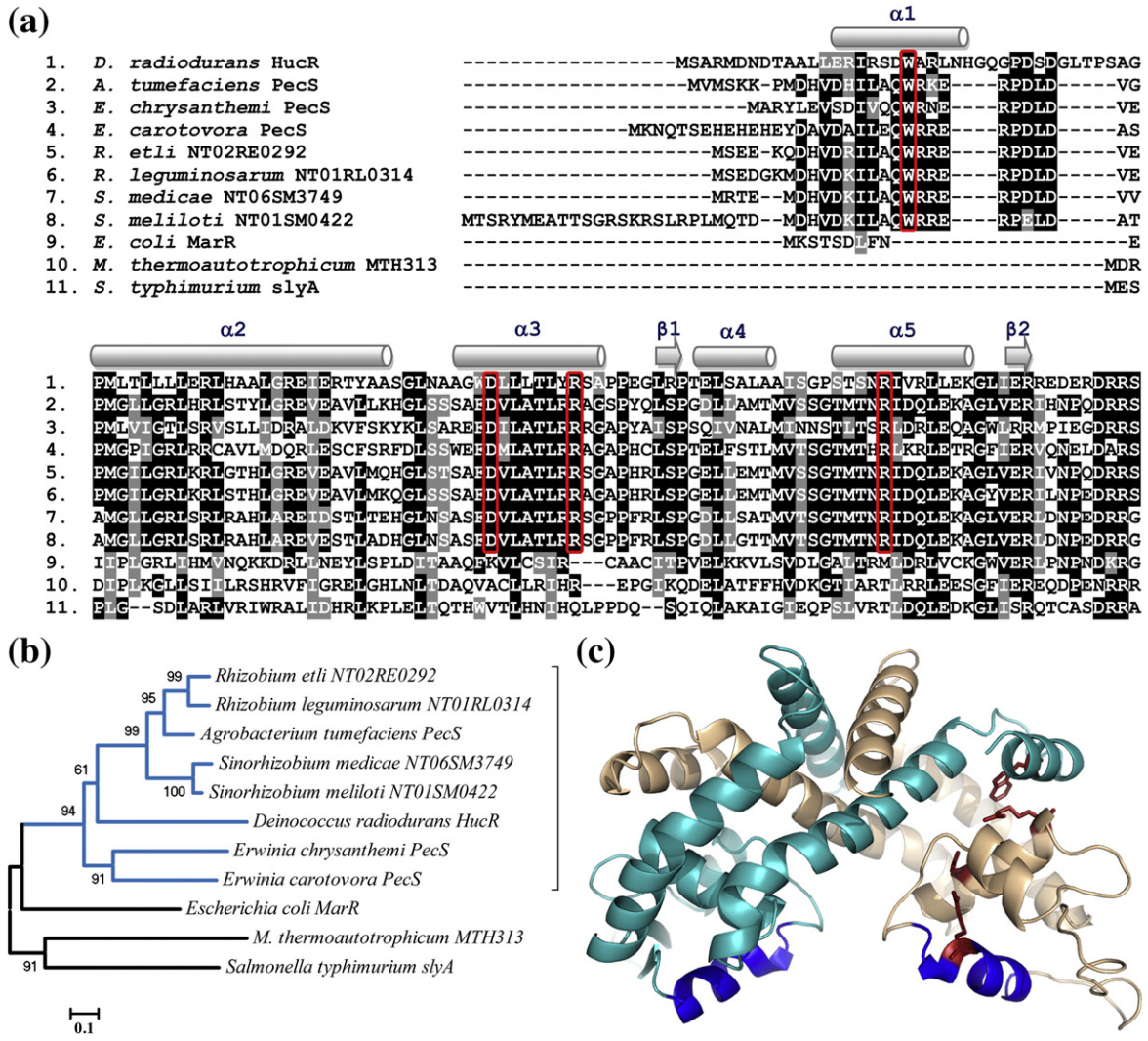

Fig. 1. (a) Sequence alignment of HucR and homologs encoded by plant pathogens. Residues involved in coordinating urate in HucR or in communicating its binding to the recognition helix are enclosed in red boxes. Secondary structure elements are from the structure of HucR;[30] N-terminal helix α1 is absent in other MarR structures. Note that, in this figure, sequences are truncated from the C-termini. (b) Phylogenetic analysis of selected MarR homologs deduced from an analysis of amino acid sequences. A phylogenetic tree was constructed by neighbor joining, where gaps were excluded. The tree was drawn to scale, and the scale bar represents an evolutionary distance of 0.1 amino acid substitution per position in the sequence. (c) Modeled structure of PecS. Each monomer (in teal and light pink) is modeled on chains A and B of HucR, respectively. DNA binding domains are shown in blue, while residues predicted to bind urate and to transmit the urate binding signal to the recognition helix are shown in red (stick representation).

the divergently oriented *pecS* and *pecM* genes. However, in electrophoretic mobility shift assays, PecS was unable to form a stable complex with DNA containing this complete palindrome (data not shown). Instead, it has a high affinity for a 190 bp fragment, including also an adjacent double overlapping pseudo-palindrome (ψ2pal) with an apparent dissociation constant (K_d) of 0.41±0.03 nM (Fig. 3a and c). PecS–*pecO* (190 bp) association is specific, as shown by complete retention of the complex during competition with >1000-fold excess binding site equivalents of nonspecific DNA. Titrating the PecS–*pecO* (190 bp) complex with DNA containing only the complete palindromic sequence (50 bp) shows that it can compete for binding to the 190 bp duplex, albeit not as efficiently as the 190 bp DNA, suggesting that PecS does bind DNA with a single palindromic sequence in solution (Fig. 3b). The interaction between PecS and *pecO* appears modestly cooperative with a Hill coefficient of 1.16±0.04 (Fig. 3c); the double-reciprocal plot shows an upward curvature consistent with positive cooperativity. This was further evidenced by the convex curvature of a Scatchard plot (data not shown). While a PecS

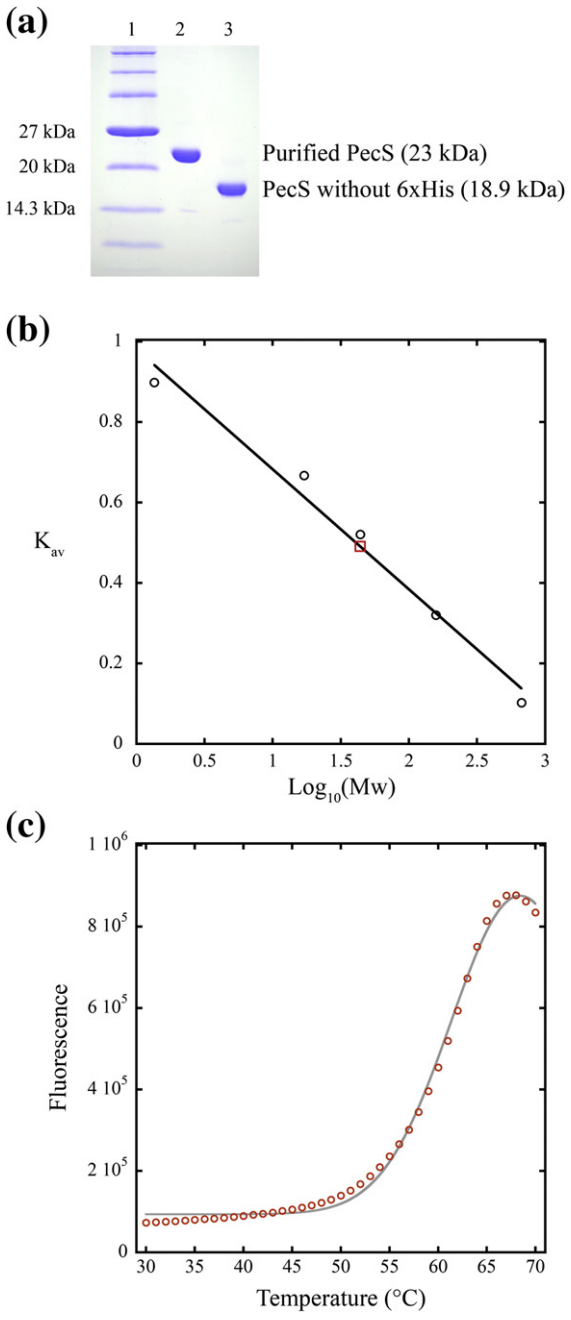

Fig. 2. PecS was purified to >95% purity. (a) Purified PecS was electrophoresed on a 15% SDS-PAGE gel: lane 1, molecular weight marker; lane 2, 5 μg of PecS; lane 3, 5 μg of PecS after cleavage of 6× His tag. (b) Gel-filtration analysis of PecS against molecular weight standards. The K_{av} of molecular weight standards (black open circles) and PecS (red open square) was graphed against the logarithm of molecular weight. (c) Melting temperature of PecS determined by differential scanning fluorometry. The fluorescence emitted from SYPRO Orange upon binding to denatured protein is measured as a function of temperature. Fluorescence is reduced after it reaches the maximum; this may be a result of the aggregation of denatured protein and dye, causing quenching.

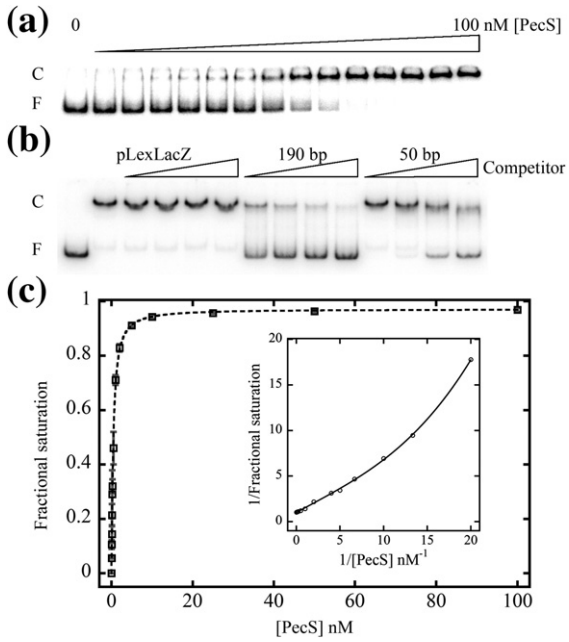

Fig. 3. Electrophoretic mobility shift assays showing DNA binding and specificity of PecS. (a) PecS binding to a 190 bp fragment of the shared operator region (PecO) of PecS and PecM; complex (C) and free DNA (F) identified on the left. (b) PecS (10 nM dimer) binding to PecO (1 nM) challenged with increasing concentrations (5–20 nM) of nonspecific plasmid DNA (pLexLacZ), 190 bp *pecO*, or 50 bp (50–500 nM) fragment containing only the perfect palindromic sequence. (c) Fractional complex formation with 190 bp PecO plotted as a function of PecS concentration. Inset: Double-reciprocal plot.

complex with DNA containing only the complete palindrome is not stable to electrophoresis, PecS forms a stable complex with DNA representing the overlapping pseudo-palindromic sequence (ψ2pal) (Fig. 4a).

DNase I footprinting confirms that PecS protects a region spanning the two identified sequences (Fig. 5). On the forward strand (with respect to *pecM*), PecS protects DNA bases 17–39 and 50–92, counting from the first base of the start codon of *pecS*, including the perfect and overlapping pseudo-palindromes, respectively. With respect to the footprint on the reverse strand, protection is shifted towards *pecS* (Fig. 5d). The extent of protection in the ψ2pal region suggests that two PecS molecules may associate. Indeed, titration of ψ2pal DNA with PecS under stoichiometric conditions shows that it binds two PecS molecules (Fig. 4). Consistent with cooperative binding, protection of both sites occurs simultaneously (Fig. 5a). Notably, protection of the overlapping palindromic sequence extends well into the coding region of *pecM*. Considering that the centers of the overlapping palindromes are 15 bp apart, our data suggest that two PecS dimers bind

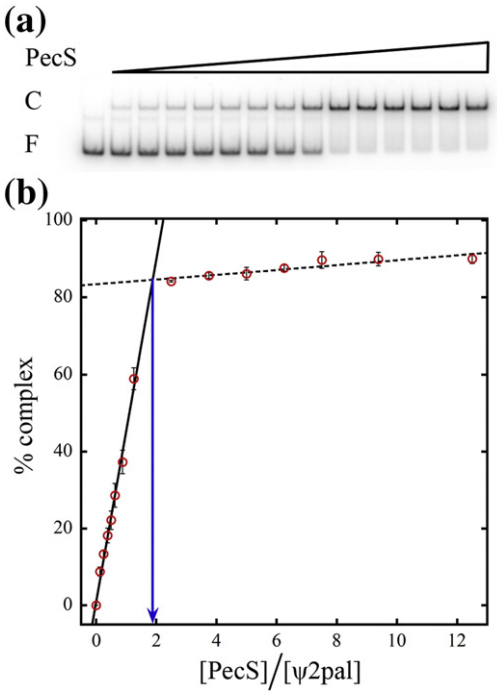

Fig. 4. PecS–ψ2pal binding stoichiometry. (a) Increasing concentrations of PecS (dimer) were incubated with 100 nM ψ2pal, and the complexes were resolved on an 8% polyacrylamide gel. (b) Plot of percent complex *versus* the ratio of *pecS* concentration to ψ2pal concentration. Error bars represent the SD derived from three experiments. The blue arrow points to the calculated stoichiometry.

the ψ2pal site on opposite faces of the DNA duplex. The two protected regions are ~10 bp apart and show cleavage enhancement, suggesting altered DNA conformation.

PecS responds to urate

DNA binding by HucR is attenuated by urate and, to a lesser extent, by xanthine, its immediate precursor in the purine degradation pathway. In contrast, no effect on DNA binding was observed upon addition of hypoxanthine or allantoin.[29] Complexes of PecS and *pecO* were therefore challenged with increasing concentrations of urate, xanthine, hypoxanthine, or salicylate; the latter is a compound seen to attenuate DNA binding by several MarR homologs (Fig. 6a). Urate and xanthine attenuate DNA binding with IC_{50} values of 3.1±0.3 mM and 2.3±0.1 mM respectively, while hypoxanthine did not affect complex formation. At lower concentrations, PecS–*pecO* complex formation is significantly reduced, followed by a more gradual reduction, with <20% of the complex remaining at 25 mM urate. In contrast, incubation with xanthine reaches a plateau of ~50% complex at 12 mM xanthine, beyond which no further PecS–*pecO* complex dissociation is seen (Fig. 6b). Salicylate also shows a concentration-dependent effect on DNA binding with an IC_{50} of 7.3±0.5 mM.

PecS contains a single Trp residue located in the predicted urate binding site. As seen with HucR, the microenvironment of this residue changes upon binding of specific ligands, manifested as concentration-dependent fluorescence quenching. Analysis of fluorescence quenching as a function of ligand concentration reveals that urate and xanthine bind PecS with comparable affinities. Urate binds with K_d=8.5±2.3 μM and negative cooperativity (n_H=0.7±0.2), whereas xanthine, having a comparable K_d of 9.1±1.5 μM, does not show cooperativity (n_H=0.9±0.2) (Fig. 6c). Taken together, these data show that urate is a ligand for PecS, and that urate attenuates DNA binding *in vitro*.

To assess whether the conserved residues in the predicted ligand binding pocket, as well as the arginine that is proposed to anchor the recognition helix to the scaffold helix α3 of the DNA binding domain, indeed function in urate-mediated attenuation of DNA binding, we mutated these residues; R95 of the recognition helix is predicted to anchor the recognition helix *via* a salt bridge to D62 of α3, while W18 and R69 are predicted to contact urate directly. Replacing D62 with S and replacing R69 with S significantly lower the responsiveness of the PecS variant to urate, indicating that these residues are important for binding urate and for relaying the occupancy of the binding pocket to the recognition helix (Fig. 7a and b); while DNA binding by PecS-R69S is unaltered upon addition of urate, DNA binding by PecS-D62S is very modestly attenuated in the presence of urate. Furthermore, mutation of R69 to S does not cause a significant change in the DNA binding affinity of PecS, with an apparent dissociation constant of 0.8±0.1 nM, while mutation of D62 to S significantly lowers the affinity of PecS for its cognate DNA (K_d=3.0±0.2 nM). PecS-W18F could not be analyzed, as the mutation of W18 to F caused the protein to aggregate and bind DNA non sequence specifically (data not shown), showing that this Trp residue is important for the proper folding of PecS. As shown for HucR, R95 was found to be vital for the proper arrangement of the recognition helix; when R95 was mutated to N, PecS lost both binding affinity and specificity (Fig. 7c).

Mid-log phase cultures of *A. tumefaciens* were exposed to exogenous urate and hydrogen peroxide to evaluate their effect on the transcription of *pecS* and *pecM* genes *in vivo*. As evidenced by quantitative RT-PCR analysis, upon addition of urate, *pecS* and *pecM* transcript levels increased by 17.0±2.8-fold and 15.0±1.7-fold, respectively, while subjecting the cells to oxidative stress did not have a significant effect on transcript levels (0.5±0.2 and 0.6±0.1) (Fig. 8). This indicates that urate functions as a ligand for PecS *in vivo*, causing derepression of

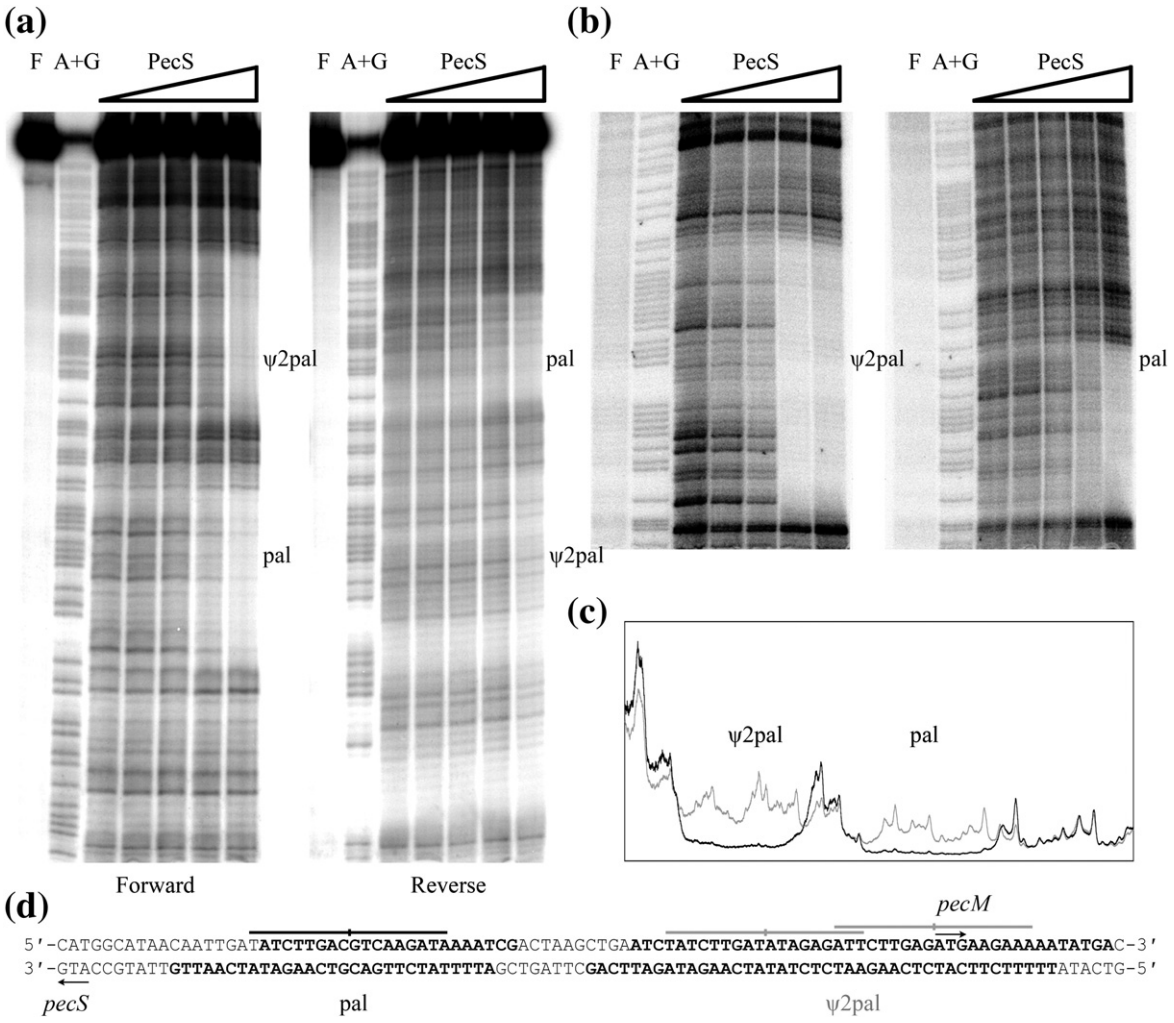

Fig. 5. DNase I footprint analysis of PecS–*pecO* interaction. (a) Forward and reverse strands are annotated with respect to the coding strand of PecM. The first lane of each subset has the undigested DNA control (F), followed by A/G chemical sequencing ladder. Increasing amounts of PecS were incubated with ^{32}P-labeled forward or reverse strands, followed by DNase I digestion. (b) Better-resolved upper protected area (ψ2pal, forward strand on the left; pal, reverse strand on the right). (c) Densitometric trace of the DNase I digest of unbound (gray) and 2 μM PecS-bound (black) forward-strand-labeled *pecO*. Protected areas are separated by ~10 bp, and cleavage enhancement between the two protected areas is visible; perfect palindromic sequence (pal) and pseudo-palindromic sequences (ψ2pal). (d) Illustration of the intergenic sequence between *pecS* and *pecM*. Start codons of the two divergently oriented genes are marked with arrows pointing in the direction of transcription. Continuous lines mark the palindromic sequences in the pal and ψ2pal regions, while the DNase-I-protected areas are shown in boldface.

both *pecS* and *pecM*. That oxidative stress does not result in elevated transcript levels suggests that urate is not produced in response to such challenge.

Discussion

Upon sensing bacterial invasion, plants upregulate an array of defense mechanisms, of which oxidative burst is among the early responses.[1,3] A primary source of oxidative radicals is xanthine oxidase, which also produces the antioxidant urate as a product.[17,34] We show here that exogenous urate causes a significantly elevated expression of *pecS* and *pecM* genes *in vivo*, and that urate mediates this effect by binding the transcriptional regulator PecS.

While PecS has been shown to be a critical regulator of infectivity and disease progression in *Erwinia*, a natural ligand for PecS has never been identified. Analysis of annotated PecS homologs reveals that all residues involved in urate binding to HucR are conserved. Furthermore, cosegregation of HucR with PecS in evolutionary tree analysis (Fig. 1b) is

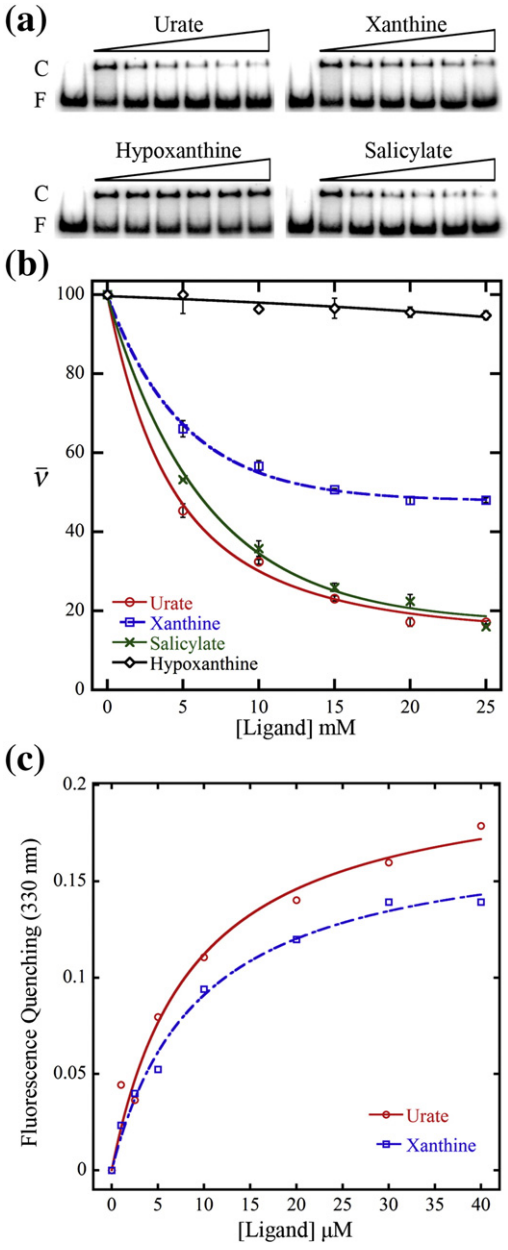

Fig. 6. (a) PecS–*pecO* complexes (C) challenged with increasing concentrations of urate, xanthine, hypoxanthine, or salicylate. The first lane of each gel, along with the corresponding parallel bands, contains a free probe (F). Note that assays are performed at high ionic strength, which is necessary to maintain the pH upon the addition of ligands dissolved in sodium hydroxide, and that the affinity of ligands is reduced at such high ionic strength. (b) Normalized PecS–*pecO* complex formation as a function of increasing ligand concentration. Error bars represent the SD of three independent experiments. (c) PecS response to urate, xanthine, and hypoxanthine. The change in intrinsic fluorescence at 330 nm was measured with an excitation of 295 nm after the addition of increasing concentrations of each ligand. The plot indicates fluorescence quenching at 330 nm as a function of ligand concentration.

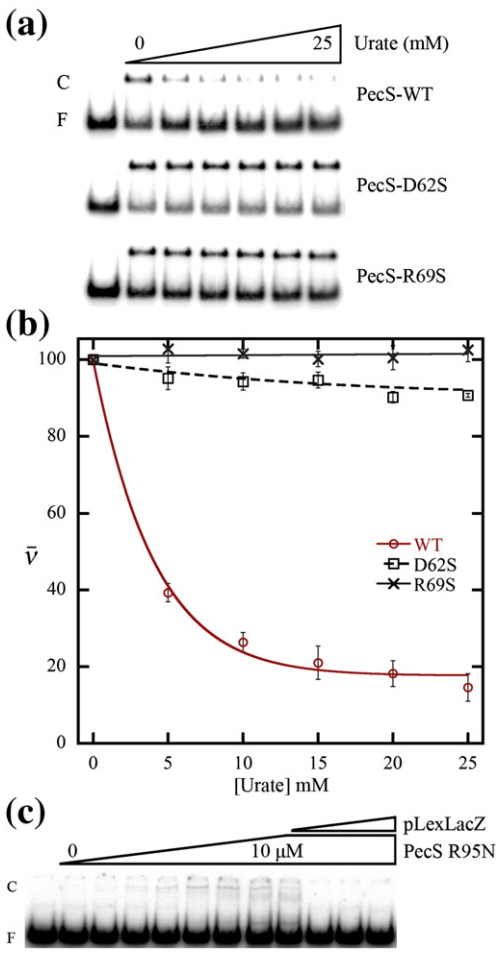

Fig. 7. DNA binding by PecS mutants. (a) Effect of urate on complex formation between PecS, PecS-D62S, and PecS-R69S, assayed by electrophoretic mobility shift assay. The first lane in each panel contains free DNA (F). (b) Normalized PecS–*pecO* complex formation as a function of increasing ligand concentration. Error bars represent the SD of three independent experiments. (c) DNA binding affinity and specificity of the PecS mutant R95N. The first lane contains free DNA (F). Increasing concentrations of nonspecific DNA (pLexLacZ) are included as indicated.

consistent with these proteins sharing a conserved mechanism of regulation that has evolved around specific effector molecules.

PecS binds multiple sites within the *pecS–pecM* region

Generally, MarR homologs bind inverted repeat sequences of 16–18 bp, and such sequences can be degenerate, as shown with SELEX (*s*ystematic *e*volution of *l*igands by *ex*ponential enrichment)-isolated sequences binding *E. chrysanthemi* PecS.[16] PecS from *A. tumefaciens* protects two regions

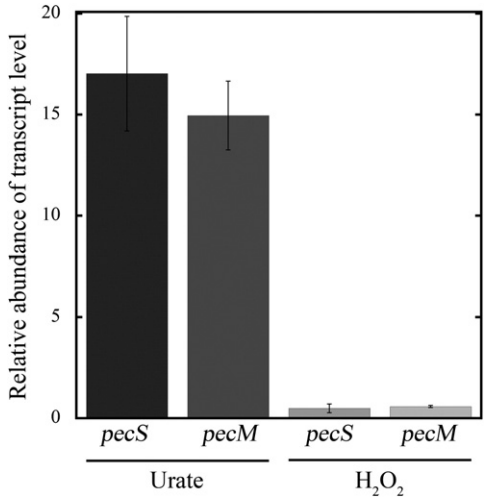

Fig. 8. Relative abundance of the transcript levels of *pecS* and *pecM* genes after the addition of 10 mM urate and 250 μM H_2O_2. mRNA levels were measured with quantitative RT-PCR, and relative abundance was calculated with comparative C_T method, with reference to the transcript level of the control group. Error bars represent the SD of three experiments.

~10 bp apart. The protected region towards *pecS* consists of a single palindromic sequence, while protection extending into the coding region of *pecM* has two overlapping pseudo-palindromic sequences (ψ2pal). Since the centers of the overlapping pseudo-palindromes are out of phase with the helical repeat, our data suggest that two PecS dimers bind on opposite faces of the double helix. As binding to the ψ2pal site appears more stable, as reflected in complexes being stable to electrophoresis, we speculate that this binding mode has evolved to ensure a more stringent control of *pecM* expression. *In vivo*, such differential expression might be manifested under conditions of limiting urate concentrations.

Urate is a ligand for PecS

That urate effects attenuated DNA binding by PecS and HucR *via* a similar mechanism is corroborated by their comparable ligand specificities. Both urate and xanthine cause a concentration-dependent disruption of the PecS–DNA complex while hypoxanthine does not; attenuated DNA binding was previously inferred to require the repulsion of conserved D73 by an N3-deprotonated ligand (a charge not present in hypoxanthine). Mutational analysis confirms that the residues proposed to be involved in the urate-mediated attenuation of DNA binding by HucR also play a vital role in the PecS response to ligands. While we were unable to analyze the W18F mutant due to its aggregation, the altered properties do indicate that W18 is necessary for the proper folding of PecS. Notably, R69S substitution abolishes the response to urate, consistent with the central prediction that R69 is important for urate binding. That binding of a negatively charged ligand is required for attenuated DNA binding is evidenced by the inability of hypoxanthine to affect DNA binding, and the inference that charge repulsion is required to bring about a conformational change in the DNA recognition helix is confirmed by the observation that a D62S mutation in PecS severely attenuates the response to urate. The residual response to urate by the PecS-D62S mutant suggests that occupancy of the binding pocket may impose minor conformational changes that translate into modestly attenuated DNA binding, even in the absence of the predicted salt bridge between D62 of the scaffold helix and R95 of the recognition helix.

Substitution of R95 results in a weak and nonspecific association with *pecO*. DNA binding by PecS appears to be more adversely affected by mutation of this residue compared to HucR; molecular modeling indicates that R95 forms the predicted salt bridge with D62, suggesting that this contact is important for anchoring the recognition helix to the scaffold helix α3. This is consistent with the lower DNA binding affinity of PecS-D62S, which would eliminate the predicted salt-bridge contact with R95. However, other contacts with residues of the recognition helix that are seen in the HucR structure may not occur in PecS; for example, a hydrophobic contact between L110 of the recognition helix and L74 of the scaffold helix in HucR may not be as favorable in PecS, which has valine in place of leucine at this position of α3 (Fig. 1). Taken together, our data indicate that the residues seen to be required for ligand-mediated attenuation of DNA binding in HucR serve equivalent functions in PecS. Furthermore, as for HucR, PecS binds urate with negative cooperativity, while binding of xanthine shows no cooperativity. This further corroborates the inference that the mechanism by which urate causes attenuated DNA binding is conserved.

Uric acid is produced by xanthine oxidase during oxidative burst in plants, triggered by invading pathogens.[35,36] Since uric acid is a potent antioxidant, plants may benefit from it in preventing extended tissue necrosis, and we speculate that the invading bacteria may exploit it to upregulate their own defense mechanisms. The observed upregulation of *pecS* and *pecM* genes by ~15-fold can be attributed to the urate-induced disruption of PecS–*pecO* interaction. Consistent with a more stable association of PecS at ψ2pal, which extends into the coding sequence of PecM, an association perhaps stabilized by protein–protein contacts, PecM levels may require tight regulation, as it may not be highly selective for the small molecules it exports.

Through transcriptomic analysis, Hommais *et al.* showed that *pecM* levels increase by ~9-fold, and that indigoidine biosynthesis genes are also upregulated upon deletion of *pecS* in *E. chrysanthemi*, indicating that PecS is directly involved in repressing these genes.[11]

Expression of *pecS* or *pecM* genes is not induced upon oxidative stress (Fig. 8). It has been previously reported that the Δ*pecS* strain of *E. chrysanthemi* is less susceptible to oxidative stress (consistent with PecS repressing the biosynthesis of the antioxidant indigoidine), and that subjecting the wild-type strain to oxidative stress upregulates indigoidine biosynthesis genes by about 4-fold.[8,11] However, this upregulation may have resulted from the low growth rate phenotype under oxidative stress, and direct regulation of *pecS–pecM* expression under these circumstances was not reported.

Salicylic acid was also able to attenuate DNA binding of PecS. Although salicylate affects DNA binding by many MarR homologs, including HucR, a physiological relevance for such phenomenon was not characterized. Salicylate is a known phytoalexin and, more interestingly, it is being investigated as an endogenous signaling molecule that upregulates the genes involved in systemic acquired resistance in plants.[37–39] In the context of *A. tumefaciens*, PecS response to salicylate may also signal the pathogen to upregulate its defense mechanisms during invasion.

In conclusion, our results show that urate is an efficient natural ligand for PecS, attenuating the binding of PecS to its operator DNA *in vitro*. Furthermore, exogenous urate causes upregulation of both *pecS* and *pecM* genes, suggesting that it can function as an efficient effector *in vivo*. Taken together, our results identify the previously elusive ligand for an important transcriptional regulator involved in controlling plant host colonization, and they suggest the possibility that urate plays a novel role in signaling such colonization.

Experimental Procedures

Sequence alignment, phylogenetic analysis, and model building

Amino acid sequences of the selected MarR homologs were aligned using Clustal W, and a neighbor-joining tree was generated with MEGA4.[40–42] Sites containing gaps were eliminated from the data set to reduce systematic errors. Confidence in neighbor joining was determined by analyzing 500 bootstrap replicates, where the percentages of replicate trees in associated taxa are shown next to branches.[43] The tree is drawn to scale; computed evolutionary distances are expressed as the number of amino acid substitutions in a site. Global alignment parameters (including gaps) were calculated according to the Needleman–Wunsch algorithm (matrix: EBLOSUM62; gap penalty: 10.0; extend penalty: 0.5) through EMBOSS:needle†.[44]

A model of *A. tumefaciens* PecS was built using SWISS-MODEL Workspace.[45] Among the available structural data for MarR homologs, the HucR structure (Protein Data Bank ID 2fbk),[30] with a 33.54% sequence identity, was automatically selected as the template. PecS monomers were separately modeled on chains A and B of HucR with minimum steric clashes, the coordinates were assembled, and the figure was generated with PyMOL.[46]

Cloning and purification

The gene encoding PecS was amplified by PCR from *A. tumefaciens* genomic DNA using the forward primer 5′-**CACC** ATG GTG ATG AGC AAG AAG AAA C-3′, which introduces the TOPO recognition sequence (the 4-bp leader is shown in boldface), and the reverse primer 5′-GAC GTA AAT CTA TTC CTC GAA GTC C-3′. The resulting PCR product was cloned into the expression vector pET100/D-TOPO (Invitrogen), which introduces an amino-terminal 6× His fusion tag, and was transformed into *E. coli* TOP-10 cells. The correct construct (named pAtPecS) was confirmed by sequencing and transformed into *E. coli* BL21(DE3)pLysS for overexpression of protein. An overnight culture started from a well-isolated single colony was diluted 1:500 in Luria–Bertani (LB) media (4 L of total volume, 250 rpm at 37 °C), and the protein was overexpressed at an OD_{600} of ~0.5 with 0.5 mM isopropyl β-D-1-thiogalactopyranoside. Induced cultures were grown for 2 h and chilled on ice for 20 min, and cell pellets harvested by centrifugation were stored at −80 °C. The cell pellets were thawed and resuspended in lysis buffer [20 mM potassium phosphate buffer (pH 7.4), 50 mM KCl, 4.5% glycerol, 10 mM imidazole, 0.15 mM phenylmethylsulfonyl fluoride (PMSF), and 10 mM 2-mercaptoethanol] and treated with 200 μg/mL lysozyme for 1 h on ice. Lysis was completed with 0.05% Triton X-100 and immediate addition of 500 mM NaCl. After a brief sonication, the suspension was spun down, and the supernatant was loaded onto a Ni-agarose column (1 mL/min). The column was washed with 10 bed volumes of lysis buffer, and the protein was eluted with a linear gradient of imidazole from 10 mM to 250 mM. The purest fractions were pooled and dialyzed overnight against HA buffer [20 mM potassium phosphate buffer (pH 7.0), 50 mM KCl, 4.5% glycerol, 0.2 mM ethylenediaminetetraacetic acid (EDTA), 0.15 mM PMSF, and 10 mM 2-mercaptoethanol] and loaded onto a heparin–agarose column equilibrated with the same buffer. After the column had been washed with 10 bed volumes of HA buffer, the protein was eluted with a linear gradient of KCl (50 mM–1 M) created with HB buffer [20 mM potassium phosphate buffer (pH 7.0), 1 M KCl, 4.5% glycerol, 0.2 mM EDTA, 0.15 mM PMSF, and 10 mM 2-mercaptoethanol]. The purest fractions were pooled, and glycerol content was raised to 20% before the fractions were flash frozen on dry ice and stored at −80 °C. Polyhistidine tag was cleaved with Enterokinase (Novagen). Five hundred micrograms of protein was incubated with 50 U of recombinant Enterokinase at room temperature for 16 h, followed by 1 h of incubation with Ni-

† http://www.ebi.ac.uk

agarose and 0.2 mM PMSF. Undigested protein and the cleaved polyhistidine tag were removed by centrifugation. The concentration of purified proteins was determined with the Micro BCA Protein Assay Kit (Pierce) using bovine serum albumin (BSA) as standard, and purity was determined by SDS-PAGE, followed by Coomassie brilliant blue staining.

PecS was mutated by whole-plasmid PCR using pAtPecS as template and the following primer pairs (5′→3′ orientation): W18F, Fw-GCG CAA TTC CGC AAG GAA CGA and Rv-GAG AAT ATG GTC GAC GTG GTC CAT; D62S, Fw-GCT TTC AGT GTG CTG GCG ACA and Rv-GGA GGA GGA GAG GCC ATG TTT TA; R69S, Fw-ACA TTG CGA AGC GCG GGC and Rv-CGC CAG CAC ATC GAA AGC G; R95N, Fw-ACA AAC AAT ATC GAC CAG CTG GAA AAA GC and Rv-CAT GGT GCC GGA GCT AAC CAT. All mutated PecS variants were overexpressed in 250 mL cultures according to the protocol for wild-type protein, except for PecS-R95N, for which cells were grown at 30 °C in 1 L of LB media starting from a freshly transformed single colony. Cells were induced at an OD_{600} of ~0.2 for 4 h at 20 °C and pelleted down. All cell pellets were disrupted by sonication in buffer Co [50 mM KCl, 4.5% glycerol, 0.15 mM PMSF, and 10 mM imidazole in 20 mM potassium phosphate buffer (pH 7.4)], followed by 30 min of centrifugation at 15,000 rpm (4 °C) to remove cell debris. Proteins were purified using TALON® Co affinity resin (Clontech). Cell lysate was incubated with the resin for 1 h, followed by an extensive washing step (>100 bed volumes) with buffer Co containing 20 mM imidazole. After the suspension had been transferred to a gravity flow column, pure protein was eluted with 500 mM imidazole in buffer Co. All mutants were purified to ~98% homogeneity; assessment of purity and storage of the protein were carried out as described above for wild-type PecS.

Gel filtration

A Superdex™-200 column (Hi load™ 16/60; GE Healthcare) with a mobile phase of 20 mM Tris (pH 7) and 150 mM NaCl was used and standardized with the following size markers: thyroglobulin, 670,000 Da; γ-globulin, 158,000 Da; ovalbumin, 44,000 Da; myoglobin, 17,000 Da; vitamin B12, 1350 Da (Bio-Rad). The K_{av} for each standard and PecS was calculated using the equation $K_{av}=(V_E-V_O)/(V_T-V_O)$, where V_E, V_O, and V_T are the retention (elution) volume of the protein, the void volume of the column, and the geometric bed volume of the column, respectively. A standard curve was obtained as a plot of K_{av} as a function of the $\log_{10}$ of molecular weight.

Protein melting temperature

PecS (5 μM) was added to a buffer with 50 mM Tris (pH 8.0), 100 mM NaCl, and 5× SYPRO Orange (Invitrogen) as reference fluorescent dye. Fluorescence emission upon binding of the dye to unfolded protein was measured over a temperature range of 5–90 °C in 1° increments for 45 s using an Applied Biosystems 7500 Real-Time PCR System (filter: SYBR green). The total fluorescence yield measured was corrected using reactions without protein. Data were analyzed with a two-state unfolding model using KaleidaGraph 4.0 (Synergy Software) with nonlinear least-squares fit, assuming that the enthalpy change between the unfolded state and the native state is constant for PecS.[47–49]

DNA binding

The *pecS–pecM* intergenic segment *pecO* was PCR amplified from *A. tumefaciens* genomic DNA with the primers *pecO*-Fw 5′-CATTGCGCGAGAATTCGGTCGA-3′ and *pecO*-Rv 5′-CAGATGGCGAATTCAAGTGC-TGTGA-3′. Five picomoles of a 190 bp DNA fragment was 5′ end labeled with [γ^{32}P]ATP and T4 polynucleotide kinase. Increasing concentrations of purified PecS were incubated, at 25 °C for 30 min, with 0.1 nM ^{32}P-labeled *pecO* in a binding buffer containing 20 mM Tris (pH 8.0), 50 mM NaCl, 0.06% BRIJ58, 20 μg/mL BSA, and 1.5% glycerol. Complexes were separated on an 8% polyacrylamide gel in 1× Tris–acetate–EDTA buffer at 7.5 V/cm (4 °C). Gels were dried under heat and vacuum, exposed to storage phosphor screens overnight, and scanned with Storm 840 PhosphorImager (GE Healthcare). Densitometric data obtained with ImageQuant 5.1 (Molecular Dynamics) were analyzed with KaleidaGraph 4.0 (Synergy Software) by fitting the binding isotherm to the Hill equation [normalized fractional saturation of *pecO*: $f=f_{max}[PecS]^n/(K_d+[PecS]^n)$, where [PecS] is the protein concentration, K_d is the apparent equilibrium dissociation constant, and n is the Hill coefficient].

The specificity of the interaction between PecS and its mutants with *pecO* was analyzed by challenging the preformed complex with a molar excess of binding site equivalents from a nonspecific plasmid pLexLacZ (Invitrogen) and by challenging the ^{32}P-labeled 190 bp *pecO*–PecS complex with unlabeled 190 bp *pecO*. The 190 bp *pecO*–PecS complex was also challenged with an increasing concentration of unlabeled 50 bp *pecO* containing only the perfect palindromic sequence.

Selected ligands were dissolved in 0.4 M NaOH. To analyze the effect of ligands on DNA binding, we used a binding buffer composed of 0.5 M Tris (pH 8.0). Binding reactions containing PecS concentrations similar to its apparent K_d and 0.2 nM ^{32}P-labeled *pecO* were challenged with increasing concentrations of urate, xanthine, hypoxanthine, or salicylate. Reactions were incubated for 30 min at room temperature, loaded onto an 8% acrylamide gel (in 50 mM Tris and 40 mM NaCl), and subjected to electrophoresis at 7.5 V/cm at 4 °C. Similarly, complexes between PecS mutants D62S and R69S and *pecO* were challenged with increasing concentrations of urate. Gels were processed and visualized as explained above. Densitometric data from three independent experiments were analyzed by nonlinear curve fitting to a two-component exponential decay.[29]

DNase I footprinting

The 190 bp PCR product for DNA binding was used with either a top strand or a bottom strand selectively end labeled by PCR amplification, using either a 5′-^{32}P-labeled forward primer or a 5′-^{32}P-labeled reverse primer. The PCR products were purified by passive elution after electrophoretic separation on an 8% polyacrylamide gel, followed by phenol–chloroform extraction and ethanol

precipitation. Binding reactions containing increasing concentrations of PecS and ~5 nM *pecO* were incubated for 30 min at room temperature (25 °C) in a binding buffer containing 20 mM Tris (pH 8.0), 50 mM NaCl, 0.06% BRIJ58, 20 μg/mL BSA, 1.5% glycerol 5 mM $MgCl_2$, and 2.5 mM $CaCl_2$ at room temperature. DNA was digested with 20 U of DNase I (New England Biolabs) for 30 s, and the reactions were terminated with an equal volume of formamide loading dye (80% deionized formamide, 10 mM EDTA, 0.1% bromophenol blue, and 1 mM NaOH). A/G chemical sequencing ladders of PecO-Fw and PecO-Rv were generated in accordance with Sambrook and Russell.[50] Samples were heated at 90 °C for 5 min before being fractionated on an 8% denaturing gel [19:1 acrylamide/bis-acrylamide, 8 M urea, and 1× Tris–borate–EDTA buffer (pH 8.3)], where the gel was prerun at ~1.5 W/cm to reach ~45 °C and run at the same wattage and temperature. After electrophoresis, the gel was dried at 80 °C under vacuum and exposed to a phosphor-imaging screen.

DNA binding stoichiometry

Complementary synthetic oligonucleotides spanning the pseudo-palindromic region on the footprint (excluding the complete palindrome) were purchased (ψ2pal), purified by denaturing gel electrophoresis followed by passive elution, and 5′ ^{32}P end labeled with [$\gamma^{32}P$]ATP and T4 polynucleotide kinase. Reactions containing 100 nM duplexed ψ2pal and increasing concentrations of PecS in a reaction buffer containing 20 mM Tris (pH 8.0), 50 mM NaCl, 0.06% BRIJ58, 20 μg/mL BSA, and 1.5% glycerol were incubated for 0.5 h, followed by electrophoretic resolution through an 8% polyacrylamide gel in 1× Tris–acetate–EDTA buffer at 7.5 V/cm. Gels, dried under heat and vacuum, were exposed to storage phosphor screens (Molecular Dynamics) and scanned with Storm 840 PhosphorImager (GE Healthcare). Data were plotted as percent complex *versus* the ratio of PecS concentration to ψ2pal concentration. The value of x at the intersection between tangents to the linear portions of the graph was calculated algebraically to obtain the stoichiometry of PecS–ψ2pal interaction upon saturation.

Tryptophan fluorescence measurement

PecS was resuspended in FL buffer [40 mM Tris–HCl (pH 8.0), 0.2 mM EDTA, 0.1% (wt/vol) BRIJ58, 100 mM NaCl, and 10 mM $MgCl_2$] to a final concentration of 0.03 mg/mL. Ligands were dissolved in 0.1 M NaOH, and reactions containing varying ligand concentrations added from an equal volume in 0.1 M NaOH were incubated for 5 min before fluorescence was measured. Emission spectrum was scanned from 300 nm to 360 nm with an excitation of 295 nm on a Jasco FP-6300 spectrofluorimeter at 25 °C using a 0.5-cm pathlength cuvette. Correction for inner filter effect, calculation of fluorescence quenching, and fitting to the Hill equation were carried out as described previously.[26]

In vivo response to urate

Overnight culture of *A. tumefaciens* was diluted 1:100 in fresh 2× LB [2% (wt/vol) tryptone, 1% (wt/vol) yeast extract, and 1% (wt/vol) NaCl] and challenged with either urate or H_2O_2 at final concentrations of 10 mM and 250 μM, respectively. Cells were harvested by centrifugation after 30 min, followed by isolation of total RNA with illustra RNAspin Mini Isolation Kit (GE Healthcare). cDNA was prepared from 2 μg of total RNA with AMV reverse transcriptase in accordance with Sambrook and Russell, and quantitative PCR was carried out with an Applied Biosystems 7500 Real-Time PCR system.[50] *pecS*, *pecM*, and the internal control gene *rpoA* were amplified with specific primers using SYBR green I fluorescence as amplification reporter. Necessary controls and validations had been carried out before the comparative C_T ($2^{-\Delta\Delta C_T}$) method was applied for data analysis.[51]

Acknowledgements

We thank Dr. Sue Bartlett for the *Agrobacterium* strain and insightful discussions, Dr. Marcia Newcomer for the use of fast protein liquid chromatography, and Nathan Gilbert and Cory Lacrouts for help with size-exclusion chromatography. National Science Foundation grant MCB-0744240 (A.G.) and a Louisiana State University Faculty Research Grant are gratefully acknowledged.

References

1. Bolwell, G. P., Bindschedler, L. V., Blee, K. A., Butt, V. S., Davies, D. R., Gardner, S. L. *et al.* (2002). The apoplastic oxidative burst in response to biotic stress in plants: a three-component system. *J. Exp. Bot.* **53**, 1367–1376.
2. Vranová, E., Inzé, D. & Van Breusegem, F. (2002). Signal transduction during oxidative stress. *J. Exp. Bot.* **53**, 1227–1236.
3. Yoshioka, H., Bouteau, F. & Kawano, T. (2008). Discovery of oxidative burst in the field of plant immunity: looking back at the early pioneering works and towards the future development. *Plant Signaling Behav.* **3**, 153–155.
4. Martinez-Romero, E. (2009). Coevolution in *Rhizobium*–legume symbiosis? *DNA Cell Biol.* **28**, 361–370.
5. Soto, M. J., Sanjuan, J. & Olivares, J. (2006). Rhizobia and plant-pathogenic bacteria: common infection weapons. *Microbiology*, **152**, 3167–3174.
6. Starr, M. P., Cosens, G. & Knackmuss, H. J. (1966). Formation of the blue pigment indigoidine by phytopathogenic *Erwinia*. *Appl. Microbiol.* **14**, 870–872.
7. Praillet, T., Reverchon, S. & Nasser, W. (1997). Mutual control of the PecS/PecM couple, two proteins regulating virulence-factor synthesis in *Erwinia chrysanthemi*. *Mol. Microbiol.* **24**, 803–814.
8. Reverchon, S., Rouanet, C., Expert, D. & Nasser, W. (2002). Characterization of indigoidine biosynthetic genes in *Erwinia chrysanthemi* and role of this blue pigment in pathogenicity. *J. Bacteriol.* **184**, 654–665.

9. Rouanet, C. & Nasser, W. (2001). The PecM protein of the phytopathogenic bacterium *Erwinia chrysanthemi*, membrane topology and possible involvement in the efflux of the blue pigment indigoidine. *J. Mol. Microbiol. Biotechnol.* **3**, 309–318.
10. Collmer, A. & Keen, N. (1986). The role of pectic enzymes in plant pathogenesis. *Annu. Rev. Phytopathol.* **24**, 383–409.
11. Hommais, F., Oger-Desfeux, C., Van Gijsegem, F., Castang, S., Ligori, S., Expert, D. *et al.* (2008). PecS is a global regulator of the symptomatic phase in the phytopathogenic bacterium *Erwinia chrysanthemi* 3937. *J. Bacteriol.* **190**, 7508–7522.
12. Perera, I. C. & Grove, A. (2010). Molecular mechanisms of ligand-mediated attenuation of DNA binding by MarR family transcriptional regulators. *J. Mol. Cell Biol.* in press. doi:10.1093/jmcb/mjq021.
13. Alekshun, M. N. & Levy, S. B. (1999). Alteration of the repressor activity of MarR, the negative regulator of the *Escherichia coli* marRAB locus, by multiple chemicals *in vitro*. *J. Bacteriol.* **181**, 4669–4672.
14. Asako, H., Nakajima, H., Kobayashi, K., Kobayashi, M. & Aono, R. (1997). Organic solvent tolerance and antibiotic resistance increased by overexpression of marA in *Escherichia coli*. *Appl. Environ. Microbiol.* **63**, 1428–1433.
15. George, A. M. & Levy, S. B. (1983). Amplifiable resistance to tetracycline, chloramphenicol, and other antibiotics in *Escherichia coli*: involvement of a non-plasmid-determined efflux of tetracycline. *J. Bacteriol.* **155**, 531–540.
16. Rouanet, C., Reverchon, S., Rodionov, D. A. & Nasser, W. (2004). Definition of a consensus DNA-binding site for PecS, a global regulator of virulence gene expression in *Erwinia chrysanthemi* and identification of new members of the PecS regulon. *J. Biol. Chem.* **279**, 30158–30167.
17. del Rio, L. A., Corpas, F. J., Sandalio, L. M., Palma, J. M., Gomez, M. & Barroso, J. B. (2002). Reactive oxygen species, antioxidant systems and nitric oxide in peroxisomes. *J. Exp. Bot.* **53**, 1255–1272.
18. Becker, B. F. (1993). Towards the physiological function of uric acid. *Free Radical Biol. Med.* **14**, 615–631.
19. Hooper, D. C., Spitsin, S., Kean, R. B., Champion, J. M., Dickson, G. M., Chaudhry, I. & Koprowski, H. (1998). Uric acid, a natural scavenger of peroxynitrite, in experimental allergic encephalomyelitis and multiple sclerosis. *Proc. Natl Acad. Sci. USA*, **95**, 675–680.
20. Varela-Echavarria, A., Montes de Oca-Luna, R. & Barrera-Saldana, H. A. (1988). Uricase protein sequences: conserved during vertebrate evolution but absent in humans. *FASEB J.* **2**, 3092–3096.
21. Cox, M. M. & Battista, J. R. (2005). *Deinococcus radiodurans*—the consummate survivor. *Nat. Rev. Microbiol.* **3**, 882–892.
22. Makarova, K. S., Aravind, L., Wolf, Y. I., Tatusov, R. L., Minton, K. W., Koonin, E. V. & Daly, M. J. (2001). Genome of the extremely radiation-resistant bacterium *Deinococcus radiodurans* viewed from the perspective of comparative genomics. *Microbiol. Mol. Biol. Rev.* **65**, 44–79.
23. Mattimore, V. & Battista, J. R. (1996). Radioresistance of *Deinococcus radiodurans*: functions necessary to survive ionizing radiation are also necessary to survive prolonged desiccation. *J. Bacteriol.* **178**, 633–637.
24. Wang, P. & Schellhorn, H. E. (1995). Induction of resistance to hydrogen peroxide and radiation in *Deinococcus radiodurans*. *Can. J. Microbiol.* **41**, 170–176.
25. Wilkinson, S. P. & Grove, A. (2004). HucR, a novel uric acid-responsive member of the MarR family of transcriptional regulators from *Deinococcus radiodurans*. *J. Biol. Chem.* **279**, 51442–51450.
26. Wilkinson, S. P. & Grove, A. (2005). Negative cooperativity of uric acid binding to the transcriptional regulator HucR from *Deinococcus radiodurans*. *J. Mol. Biol.* **350**, 617–630.
27. Imhoff, R. D., Power, N. P., Borrok, M. J. & Tipton, P. A. (2003). General base catalysis in the urate oxidase reaction: evidence for a novel Thr-Lys catalytic dyad. *Biochemistry*, **42**, 4094–4100.
28. Lee, Y., Lee, D. H., Kho, C. W., Lee, A. Y., Jang, M., Cho, S. *et al.* (2005). Transthyretin-related proteins function to facilitate the hydrolysis of 5-hydroxyisourate, the end product of the uricase reaction. *FEBS Lett.* **579**, 4769–4774.
29. Perera, I. C., Lee, Y. H., Wilkinson, S. P. & Grove, A. (2009). Mechanism for attenuation of DNA binding by MarR family transcriptional regulators by small molecule ligands. *J. Mol. Biol.* **390**, 1019–1029.
30. Bordelon, T., Wilkinson, S. P., Grove, A. & Newcomer, M. E. (2006). The crystal structure of the transcriptional regulator HucR from *Deinococcus radiodurans* reveals a repressor preconfigured for DNA binding. *J. Mol. Biol.* **360**, 168–177.
31. Alekshun, M. N., Levy, S. B., Mealy, T. R., Seaton, B. A. & Head, J. F. (2001). The crystal structure of MarR, a regulator of multiple antibiotic resistance, at 2.3 Å resolution. *Nat. Struct. Biol.* **8**, 710–714.
32. Saridakis, V., Shahinas, D., Xu, X. & Christendat, D. (2008). Structural insight on the mechanism of regulation of the MarR family of proteins: high-resolution crystal structure of a transcriptional repressor from *Methanobacterium thermoautotrophicum*. *J. Mol. Biol.* **377**, 655–667.
33. Andresen, C., Jalal, S., Aili, D., Wang, Y., Islam, S., Jarl, A. *et al.* (2009). Critical biophysical properties in the *Pseudomonas aeruginosa* efflux gene regulator MexR are targeted by mutations conferring multidrug resistance. *Protein Sci.* **19**, 680–692.
34. Choi, E. Y., Stockert, A. L., Leimkuhler, S. & Hille, R. (2004). Studies on the mechanism of action of xanthine oxidase. *J. Inorg. Biochem.* **98**, 841–848.
35. Lamb, C. & Dixon, R. A. (1997). The oxidative burst in plant disease resistance. *Annu. Rev. Plant Physiol. Plant Mol. Biol.* **48**, 251–275.
36. Averyanov, A. (2009). Oxidative burst and plant disease resistance. *Front. Biosci. (Elite Edit.)*, **1**, 142–152.
37. Ward, E. R., Uknes, S. J., Williams, S. C., Dincher, S. S., Wiederhold, D. L., Alexander, D. C. *et al.* (1991). Coordinate gene activity in response to agents that induce systemic acquired resistance. *Plant Cell*, **3**, 1085–1094.
38. Reymond, P. & Farmer, E. E. (1998). Jasmonate and salicylate as global signals for defense gene expression. *Curr. Opin. Plant Biol.* **1**, 404–411.

39. Mabood, F. & Smith, D. (1997). The role of salicylates in *Rhizobium*–legume symbiosis and abiotic stresses in higher plants. pp. 161–163, Springer, Dordrecht, The Netherlands.
40. Tamura, K., Dudley, J., Nei, M. & Kumar, S. (2007). MEGA4: Molecular Evolutionary Genetics Analysis (MEGA) software version 4.0. *Mol. Biol. Evol.* **24**, 1596–1599.
41. Larkin, M. A., Blackshields, G., Brown, N. P., Chenna, R., McGettigan, P. A., McWilliam, H. *et al.* (2007). Clustal W and Clustal X version 2.0. *Bioinformatics*, **23**, 2947–2948.
42. Saitou, N. & Nei, M. (1987). The neighbor-joining method: a new method for reconstructing phylogenetic trees. *Mol. Biol. Evol.* **4**, 406–425.
43. Sanderson, M. J. & Wojciechowski, M. F. (2000). Improved bootstrap confidence limits in large-scale phylogenies, with an example from Neo-Astragalus (Leguminosae). *Syst. Biol.* **49**, 671–685.
44. Needleman, S. B. & Wunsch, C. D. (1970). A general method applicable to the search for similarities in the amino acid sequence of two proteins. *J. Mol. Biol.* **48**, 443–453.
45. Bordoli, L., Kiefer, F., Arnold, K., Benkert, P., Battey, J. & Schwede, T. (2009). Protein structure homology modeling using SWISS-MODEL Workspace. *Nat. Protoc.* **4**, 1–13.
46. DeLano, W. L. (2008). *The PyMOL Molecular Graphics System.* DeLano Scientific, Palo Alto, CA.
47. Ramsay, G. D. & Eftink, M. R. (1994). Analysis of multidimensional spectroscopic data to monitor unfolding of proteins. *Methods Enzymol.* **240**, 615–645.
48. Koepf, E. K., Petrassi, H. M., Sudol, M. & Kelly, J. W. (1999). WW: an isolated three-stranded antiparallel beta-sheet domain that unfolds and refolds reversibly; evidence for a structured hydrophobic cluster in urea and GdnHCl and a disordered thermal unfolded state. *Protein Sci.* **8**, 841–853.
49. Niesen, F. H., Berglund, H. & Vedadi, M. (2007). The use of differential scanning fluorimetry to detect ligand interactions that promote protein stability. *Nat. Protoc.* **2**, 2212–2221.
50. Sambrook, J. & Russell, D. W. (2001). *Molecular Cloning: A Laboratory Manualpp. 7.42–7.50,* 3rd edit. Cold Spring Harbor Laboratory, Cold Spring Harbor, NY pp. 7.42–7.50.
51. Schmittgen, T. D. & Livak, K. J. (2008). Analyzing real-time PCR data by the comparative C_T method. *Nat. Protoc.* **3**, 1101–1108.